

First evidence for the detection of natural surface films by the QuikSCAT scatterometer

I.-I. Lin,¹ Werner Alpers,² and W. Timothy Liu³

Received 26 March 2003; accepted 1 May 2003; published 12 July 2003.

[1] For the first time it is demonstrated that with the QuikSCAT scatterometer it is possible to detect natural surface films resulting from enhanced biological activity in the ocean. It is shown for two regions in the Norwegian and Baltic Sea that areas of strongly reduced Normalized Radar Cross Section (NRCS) are associated with areas of enhanced chlorophyll-a concentration as evidenced by quasi-simultaneously acquired SeaWiFS data. This result has two implications. Firstly, it opens up the possibility to map globally natural surface film coverage using QuikSCAT data. Secondly, it demonstrates that in ocean areas with high biological activity the presence of natural surface films can give rise to significant errors in wind vector retrieval when using the current QuikSCAT wind retrieval algorithm. *INDEX TERMS:* 4275 Oceanography: General: Remote sensing and electromagnetic processes (0689); 4506 Oceanography: Physical: Capillary waves; 4854 Oceanography: Biological and Chemical: Physicochemical properties; 4504 Air/sea interactions (0312); 4899 General or miscellaneous. *Citation:* Lin, I.-I., W. Alpers, and W. T. Liu, First evidence for the detection of natural surface films by the QuikSCAT scatterometer, *Geophys. Res. Lett.*, 30(13), 1713, doi:10.1029/2003GL017415, 2003.

1. Introduction

[2] There is much demand to map natural surface film coverage on a global scale since natural surface films significantly affect the gas, heat, and momentum exchange between the atmosphere and the ocean [Asher, 1997; Frew, 1997; Tsai and Liu, 2003]. Natural surface films in the form of monomolecular slicks originate mainly from exudation and secretion of fish and plankton, in particular of phytoplankton [Zutic *et al.*, 1981]. They strongly damp short-scale surface waves (short gravity and capillary waves). Thus they become detectable by active microwave remote sensors because a reduction of the amplitude of short-scale waves gives rise to a reduction of the Normalized Radar Cross Section (NRCS) [Alpers and Hühnerfuss, 1989]. Although the detection of slicks by space-borne Synthetic Aperture Radars (SARs) is well reported [Alpers and Hühnerfuss, 1989], their narrow swath (typically 100–500 km) and their long revisit time (typically 24–35 days) inhibit the mapping of slick coverage on a global scale within a reasonable timeframe. Since the QuikSCAT scatterometer has a 1,800 km swath covering 93% of the global

ocean daily [Liu *et al.*, 1998], it would be highly desirable to use QuikSCAT data in performing such a task. However, it has been unclear whether the Ku band (13.4 GHz) QuikSCAT scatterometer is sufficiently sensitive to slicks because of two reasons. Firstly, only limited airborne Ku-band scatterometer data acquired over ocean areas covered with surface films exist [Hühnerfuss *et al.*, 1978; Hühnerfuss *et al.*, 1996; Gade *et al.*, 1998], and secondly, the QuikSCAT scatterometer has a much coarser spatial resolution (25 km) than the space-borne SARs (25 m or less).

[3] This paper is a first report of our systematic investigation on world-wide slick detection by using QuikSCAT data. Here we present two examples: one from the Norwegian Sea at the northeast of Iceland and one from the Baltic Sea. In both cases the data were acquired during the spring phytoplankton bloom (period of high biological activity). In addition to QuikSCAT data, we also use co-located and nearest-coincident chlorophyll-a concentration (Chl-a) data from the SeaWiFS sensor (Sea-viewing Wide Field-of-view Scanner) and Sea Surface Temperature (SST) data from the NOAA/Advanced Very High Resolution Radiometer (AVHRR). Also, operational analysis surface wind vector and air temperature data from the European Centre for Medium Range Weather Forecast (ECMWF) and the US National Centers for Environmental Prediction (NCEP) are jointly-analysed.

2. Methodology

[4] We compare first sea surface wind vectors derived from QuikSCAT with the nearest co-incident NCEP or ECMWF reanalysis sea surface wind vectors. For this comparison it is essential that no scatterometer data, e.g., from QuikSCAT or the European Remote Sensing Satellites (ERS-1 and 2), has been assimilated into the reanalysis wind vector data. Thus for the first case study, the Norwegian Sea case on 6 May 2000, we use NCEP wind vector data and for the second case study, the Baltic Sea case on 23 May 2001, we use ECMWF wind vector data.

[5] Since in slick areas the NRCS is reduced, the sea surface wind speed derived from QuikSCAT should be lower there than the reanalysis wind speed. Taking the reanalysis data as reference, the areas where QuikSCAT underestimates the wind speed are thus identified as potential slick-covered areas. Once these areas are identified, the reanalysis wind field is used as input to the forward QuikSCAT model function (from QuikSCAT Project) to generate a simulated NRCS map. This simulated QuikSCAT NRCS map thus represents the NRCS map to which only the sea surface wind field contributes. In contrast to this, the measured QuikSCAT NRCS map contains also contributions from the slicks. By subtracting both NRCS maps, we

¹National Center for Ocean Research, Taipei, Taiwan.

²Institute of Oceanography, University of Hamburg, Germany.

³Jet Propulsion Laboratory, NASA, USA.

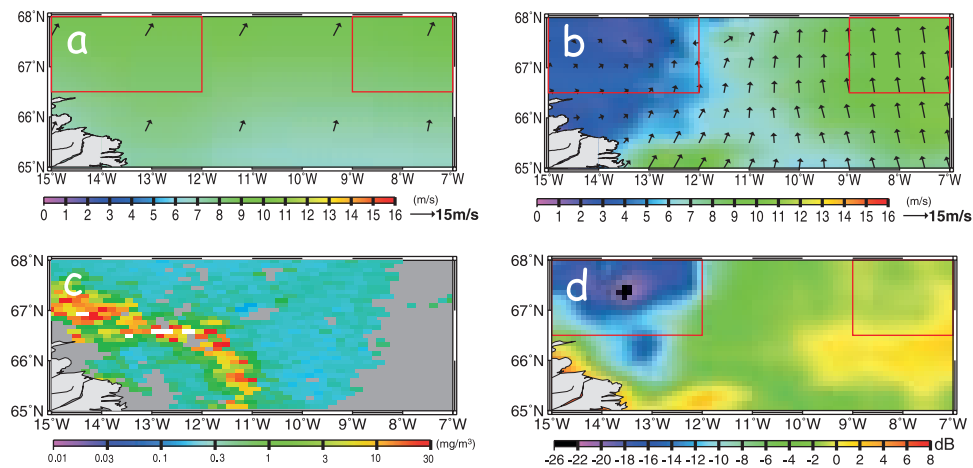


Figure 1. (a) NCEP Sea surface wind field map of the Norwegian Sea case at 06:00 UTC, 6 May 2000. (b) QuikSCAT sea surface wind field map for the same day, but at 05:43 UTC. (c) Map of the chlorophyll-a concentration from SeaWiFS passes at 13:37 UTC and 15:16 UTC of the same day. (d) NRCS difference map obtained by subtracting the QuikSCAT-measured NRCS map (supfig1b)¹ from the simulated NRCS map (supfig1a)¹.

obtain the difference map, which is used to locate the slick-covered areas.

[6] QuikSCAT uses two pencil-beam antennas: the inner beam operates at an incidence angle of 46 degrees and at horizontal polarization and the outer one at an incidence angle of 54 degrees and at vertical polarization. Since the antennas are conically scanning [Liu *et al.*, 1998], a resolution cell on the ocean surface, called wind vector cell (WVC), is, in general, viewed by each beam from two different azimuth directions: the first time when looking forward (fore) and the second time when looking aft. Thus four NRCS maps can be generated which differ in polarization, incidence angle, and look direction. The difference NRCS maps are then compared with the collocated/nearest co-incident SeaWiFS chlorophyll-a map (spatial resolution: 4km) to check whether areas of reduced NRCS values are associated with high chlorophyll-a concentrations. To exclude other factors that potentially also can cause an NRCS reduction, we compare the NRCS difference map with the QuikSCAT rain flag map, the nearest coincident NOAA/AVHRR SST map, and the air-sea temperature difference map (derived from the analysis air temperature map and AVHRR SST map).

3. Results: Norwegian Sea Case

[7] Figure 1a shows the NCEP sea surface wind field over the Norwegian Sea on 6 May 2000 at 06:00 UTC and Figure 1b the QuikSCAT wind field on the same day at 05:43 UTC. The co-located/nearest-coincident chlorophyll-a map from a composite of SeaWiFS passes on 6 May 2000 is depicted in Figure 1c. Figure 1d shows the difference between the QuikSCAT-measured NRCS map (supfig1b)¹ and the NCEP-wind simulated NRCS map (supfig1a)¹ for the aft-looking outer beam. When comparing the NCEP wind field (Figure 1a) with the one retrieved from QuikSCAT (Figure 1b), large differences can be delineated in certain areas. In the western section (66–68°N, 12–15°W), the QuikSCAT wind speed (Figure 1b) is in the range between

2–4 m/s (colour coded: purple to dark blue), which is 3–7 m/s lower than the corresponding NCEP wind speed of 7–9 m/s (colour coded: green) (Figure 1a). On the other hand, in the eastern section (65–68°N, 7–11°W) the QuikSCAT wind speed is similar to the NCEP wind speed, both have values between 7 and 9 m/s (colour coded: green). Such differences are also visible in the corresponding NRCS difference map (Figure 1d). Significant reduction of the NRCS (–14 to –26 dB, colour coded: blue-purple) is clearly visible in the western section, while in the eastern section the NRCS difference is small, typically between –2 and 2 dB (colour coded: green-yellow).

[8] Examine the Chl-a map (Figure 1c), intense phytoplankton bloom patch, characterised by high Chl-a concentration of predominantly 8–30 mg/m³ (colour coded: yellow-orange-red) is found in the western section. In the eastern section, Chl-a concentration is very low (≤ 0.3 mg/m³, colour coded: light blue-blue). This supports that the reduction of the NRCS in the western section is caused by slicks resulting from high biological activity in this area. We also observe that the area with reduced NRCS is larger than the area with increased chlorophyll-a concentration where the surplus slick-covered area is found at NNE from the intensified phytoplankton bloom area. This is expected, because the prevailing wind from SSW (Figure 1a) blows the slick out of the source region. Thus the slick is spread over a wider region in the direction of the wind (66–68°N, 12–15°W).

[9] Since the NRCS is reduced in slick-covered areas, the wind speed derived from the QuikSCAT-measured NRCS data by using the standard QuikSCAT model function is underestimated. This is shown quantitatively in Figure 2, where for each wind vector cell within the two boxes marked in Figures 1a, 1b, and 1d the wind speed difference (QuikSCAT wind speed minus NCEP wind speed) is plotted versus the NRCS difference (measured QuikSCAT NRCS minus simulated QuikSCAT NRCS). It is clearly seen that at the slick-covered area (western box, symbol: filled-triangle), the underestimation of the wind speed is between 3 and 7 m/s, while in the slick-free area (eastern box, symbol: Δ) the NCEP and QuikSCAT wind speeds are almost the same (0 to 2 m/s difference).

¹ Auxiliary material is available at <ftp://agu.org/apend/gl/2003GL017415>.

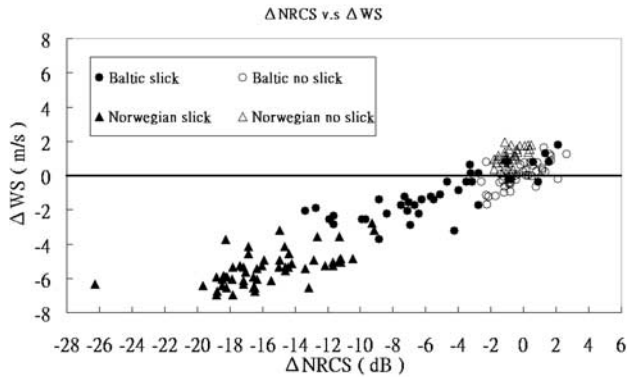


Figure 2. NRCS difference (X-axis) against QuikSCAT wind speed underestimation error (Y-axis) for slick-covered (Norwegian Sea Case, symbol: filled-triangle; Baltic Sea case: ●) and non-slick covered (Norwegian Sea Case: △; Baltic Sea case: ○) areas (box location depicted in Figures 1a, 1b, 1d, 3a, 3b, 3d).

[10] In order to corroborate our hypothesis that the reduction of the NRCS in the western section is indeed caused by the presence of slicks, and not by spatial variations of the SST or by the air-sea temperature difference (stability of the air-sea interface), or by the presence of rain, we have compared the NRCS difference map with the nearest co-incident SST and air-sea temperature difference maps as well as the QuikSCAT rain flag map (supfig2 and supfig3)¹. In the slick-covered area the SST (supfig2a)¹ is approximately 1–2°C higher than in the slick-free area and the air-sea temperature difference (supfig2b)¹ is here slightly negative (0 to –1°C, colour coded: blue-purple) indicating a slightly unstable air-sea interface. Both effects, the increase of the SST (a well-known effect over slick-covered areas) [Alpers, 2001] and the increase of the air-sea temperature difference in the slick-covered areas, should rather cause an increase of the NRCS than a decrease. Furthermore, the QuikSCAT rain flag map (supfig3)¹ reveals that no rain was present. All these facts lend support to our hypothesis that the reduction of the NRCS in the western section of the analyzed area is caused by the presence of slicks associated with enhanced biological activity.

4. Results: Baltic Sea Case

[11] Now we carry out a similar analysis for the Baltic Sea as for the Norwegian Sea. Figure 3a shows the ECMWF sea surface wind field over the Baltic Sea on 23 May 2001 at 18:00 UTC and Figure 3b the QuikSCAT wind field on the same day at 16:57 UTC. The co-located/nearest-incident chlorophyll-a map from a composite of SeaWiFS passes between 23 and 24 May 2001, is depicted in Figure 3c. Figure 3d shows the difference between the NRCS maps from the measured (supfig4b)¹ and the simulated NRCS map (supfig4a)¹ for the aft-looking outer beam. Figure 3c shows in the northern section of the Baltic Sea (58–66°N, 17–25°E), high chlorophyll-a concentration (4–8 mg/m³, colour coded: orange-red) and in the southern section (54–57°N, 15–22°E) lower concentration (1–3 mg/m³, colour coded: green-yellow). By comparing Figure 3c with Figure 3d we see that areas of high chlorophyll-a concentration in the

Northern Baltic Sea (e.g., 64–66°N, 22–25°E and 60–63°N, 18–22°E) correlate well with areas of large NRCS reduction (–4 to –12 dB, colour coded: blue-purple). In the Southern Baltic Sea (54–57°N, 15–22°E), the chlorophyll-a concentration is much lower and the wind much stronger (9–10 m/s, colour coded: orange-red in Figure 3a). The lower the chlorophyll-a concentration and thus less slicks present, and the stronger the wind (slicks are washed down by breaking waves), the smaller is the reduction of the NRCS (close to 0 dB, colour coded: green in Figure 3d).

[12] However, it is very likely that the slick-covered areas encountered in the northern Baltic Sea consist not only of natural slicks, but also partly of man-made slicks. They have their origin in the direct inflow of surface-active material from municipal and industrial plants located in Baltic states and in Russia. Additional nutrients (e.g., fertilizers from agricultural lands) are deposited into the sea which leads to eutrophication and thus increase in algae growth and slick production. These man-made slicks have a similar effect on the air-sea gas, heat, and momentum exchange as the natural slicks.

[13] Like in the Norwegian Sea case, the reduction of the NRCS leads to an underestimation of the wind speed. This is shown quantitatively in Figure 2 for the two boxes marked in Figures 3a, 3b, and 3d representing a slick-covered area (60.6–62.7°N, 18.8–20.7°E) area and a slick-free area (55.3–56.4°N, 16.9–20.5°E). In the slick-covered area (northern box, symbol: ●), the underestima-

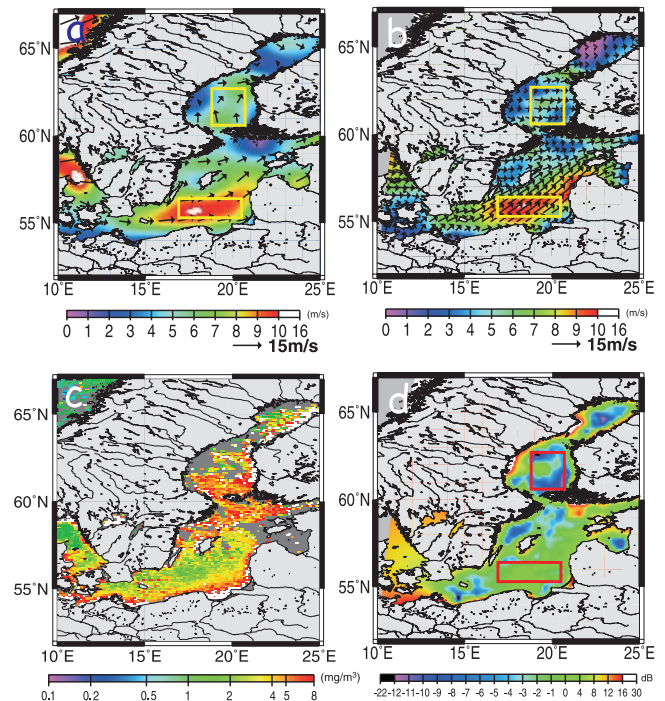


Figure 3. (a) ECMWF Sea surface wind field map of the Baltic Sea case at 18:00 UTC 23 May 2001. (b) QuikSCAT sea surface wind field map for the same day, but at 16:57 UTC. (c) Map of the chlorophyll-a concentration from SeaWiFS passes on 23–24 May 2001. (d) NRCS difference map obtained by subtracting the QuikSCAT-measured NRCS map (supfig4b)¹ from the simulated NRCS map (supfig4a)¹.

tion of the wind speed is between 1 and 4m/s while in the slick-free area (southern box, symbol: ○), it is nearly zero. In order to exclude that SST, air-sea temperature difference, and rain effects are causing the observed NRCS reduction, we have carried out the same analysis as described for the Norwegian Sea case. We have found no indications that they had any effect on the NRC reduction (supfig4–6)¹.

5. Conclusion

[14] It is well known that imaging radars can be used for detecting small to medium-scale slicks which have dimensions from some tens of meters to tens of kilometers [Alpers and Hühnerfuss, 1989], but till now it has not been realized that spaceborne scatterometers can be used for detecting large-scale slicks which have dimensions of several hundred kilometers and thus have the potential to carry out global measurements of slick coverage. In this paper we have presented evidence that indeed scatterometers can be used for this task. We have demonstrated this in two case studies by using synergy data comprising QuikSCAT, SeaWiFS, AVHRR, and operational analysis meteorological data from weather service centers. The QuikSCAT data shows a strong reduction of the Normalized Radar Cross Section(NRCS) (6–20 dB) in areas where the SeaWiFS data show a high chlorophyll-a concentration (≥ 4 mg/m³).

[15] We attribute the reduction of the NRCS primarily to the presence of sea slicks produced by biogenic processes in the ocean. As already suggested by Garrett [1986], natural slick coverage can be used as a proxy for ocean productivity. Unlike ocean colour sensors, which provide data only during the day when there are no clouds, scatterometers yield data also at night and in the presence of clouds and are thus suited for global measurements. Since surface films have a strong impact on the carbon dioxide flux from the atmosphere into the ocean and vice versa [Frew, 1997], estimates of the global distribution of natural sea slicks derived from spaceborne scatterometer data are of value in climate studies concerned with the carbon cycle. Finally, the knowledge of the global distribution of sea slicks is also essential for improving the algorithm for retrieving sea surface wind vectors from scatterometer data. As shown in this paper, the errors in the wind speed inferred from QuikSCAT data when using the standard wind retrieving scheme (i.e., neglecting the influence of slicks) can be as high as 7 m/s. The QuikSCAT wind vector error induced by

rain has already been investigated in detail [Huddleston and Stiles, 2000], but so far not the error induced by slicks discussed in this paper. Therefore more attention should be given to slick-induced effects when aiming at improving the wind retrieval algorithms for the QuikSCAT and other scatterometers.

[16] **Acknowledgments.** The authors wish to thank Drs. Wu-Ting Tsai and Kon-Kee Liu for helpful discussions and to Drs. Wen-der Liang, Chun-Chieh Wu, Ms. Meggie Lien, and Mr. Faye Pan for help in data provision and processing. This work was performed while one of us (W.A.) was a Visiting Professor at NCOR.

References

- Alpers, W., Air-sea interaction: Surface films, in *Encyclopedia of Ocean Sciences*, Academic Press, London, UK, 2001.
- Alpers, W., and H. Hühnerfuss, The damping of ocean waves by surface films: A new look at an old problem, *J. Geophys. Res.*, *94*, 6251–6265, 1989.
- Asher, W. E., The sea-surface microlayer and its effects on global air-sea gas transfer, in *The Sea Surface and Global Change*, edited by P. S. Liss and R. A. Duce, 251–286, Cambridge University Press, 1997.
- Frew, N. M., The role of organic films in air-sea gas exchange, in *The Sea Surface and Global Change*, edited by P. S. Liss and R. A. Duce, Cambridge University Press, 1997.
- Gade, M., W. Alpers, H. Hühnerfuss, V. R. Wismann, and P. A. Lange, On the reduction of the radar backscatter by oceanic surface films: scatterometer measurements and their theoretical interpretation, *Remote Sens. Environ.*, *66*, 52–70, 1998.
- Garrett, W. D., Physicochemical effects of organic films at the sea surface and their role in the interpretation of remotely sensed imagery, *ONRL Workshop Proceedings: Role of Surfactant Films on the Interfacial Properties of the Sea Surface*, edited by F. L. Herr and J. Williams, Office of Naval Research, London Branch, ONRL Report, C-11-86, 1–17, 1986.
- Huddleston, J. N., and B. W. Stiles, Multidimensional Histogram (MUDH) rain flag product description, version 2.1, Jet Propulsion Laboratory, Pasadena, CA, 2000.
- Hühnerfuss, H., W. Alpers, and W. L. Jones, Measurements at 13.9 GHz of the radar backscattering cross section of the North Sea covered with an artificial surface film, *Radio Science*, *13*, 979–983, 1978.
- Hühnerfuss, H., W. Alpers, H. Dannhauer, M. Gade, P. A. Lange, V. Neumann, and V. Wismann, Natural and man-made sea slicks in the North Sea investigated by a helicopter-borne 5-frequency radar scatterometer, *Int. J. Remote Sensing*, *17*, 1567–1582, 1996.
- Liu, W. T., W. Tang, and P. S. Polito, NASA Scatterometer provides global ocean-surface wind fields with more structures than numerical weather prediction, *Geophys. Res. Lett.*, *25*, 761–764, 1998.
- Tsai, W. T., and K. K. Liu, An assessment of the effect of sea surface surfactant on global atmosphere-ocean CO₂ flux, *J. Geophys. Res.*, in press, 2003.
- Zutic, V., B. Cosovic, E. Marcenko, N. Bihari, and F. Krsinic, Surfactant production by marine phytoplankton, *Marine Chemistry*, *10*, 505–520, 1981.

I.-I. Lin, National Center for Ocean Research, P.O. Box 23-13, Taipei, 10617, Taiwan. (linii@ncor.ntu.edu.tw)